Absorptions and Emissions for the $TmCl_6^{3-}$ Ion in $Cs_2NaTmCl_6$

R. Acevedo[a,*], O.F. Hurtado[a], C. Portillo[a] and W. Stręk[b]

[a]Departamento de Quimica Basica, Facultad de Ciencias Fisicas y Matematicas
Universidad de Chile, Beauchef 850, Casilla 2777, Santiago-Chile
[b]Institute of Low Temperature and Structure Research
Polish Academy of Sciences
Okólna 2, 50-422 Wrocław, Poland

(Received March 5, 2001; revised version October 18, 2001)

In this work we report both experimental and theoretical studies regarding the $Cs_2NaTmCl_6$ elpasolite-type system, for which we have an updated database from linear and nonlinear optics. Both the absorption and the emission spectra for this system are rather complicated and a generalized vibronic crystal field-closure-ligand polarization calculation model has been employed to rationalize the observed spectral intensities. The calculation has been carried out by neglecting the interaction among the internal and the external vibrations and theoretical calculations have been performed with reference to both the emissions $^3H_4(\Gamma_i) \rightarrow {}^3F_4(\Gamma_j)$ and the absorptions $^3H_6(A_1) \rightarrow {}^3F_4(\Gamma_i)$, $^1G_4(\Gamma_i)$, $^3H_5(\Gamma_l)$ with Γ_k $(k = i, j) = A_1, E, T_1, T_2$ and $\Gamma_l = E, {}^aT_1, {}^bT_1, T_2$. The advantages and disadvantages of our model calculation are discussed in the text, and despite the simplicity of the model it is shown that it has got some utility and flexibility to gain understanding in these complex phenomena.

PACS numbers: 32.70.Fw

1. Introduction

The main goal of the current research work is to report both experimental and theoretical studies, regarding luminescence materials of the elpasolite-type system, such as $Cs_2NaLnCl_6$, for which an updated database has become available

*corresponding author; e-mail: lindsey@cec.uchile.cl

from linear and non-linear optics. These systems show very complex absorption and emission spectra and the need for developing new theoretical models is a priority so as to advance the state of the art in this area of the solid state physics. The paper has been divided into two sections; one of them devoted to some experimental aspects of both the synthesis and the structural characterization of the $Cs_2NaTmCl_6$ crystal, and the other related to the rationalization of the observed experimental data associated with both the absorptions and the emissions spectra for this system. Thus, we report the synthesis and structural characterization for this elpasolite and its crystallographic parameters, which have been refined using the Rietveld method. This new experimental data may be utilized to gain understanding of the mechanistic factors (electronic and vibrational), upon which the spectral intensities and the main spectral features depend on. Due to the complexity of both the absorptions and the emissions spectra, we have carried out theoretical calculations of the radiative processes associated with both the emissions $^3H_4(\Gamma_i) \rightarrow {}^3F_4(\Gamma_j)$ and the absorptions $^3H_6(A_1) \rightarrow {}^3F_4(\Gamma_i)$, $^1G_4(\Gamma_i)$, $^3H_5(\Gamma_l)$ with $\Gamma_k(k = i, j) = A_1, E, T_1, T_2$ and $\Gamma_l = E, {}^aT_1, {}^bT_1, T_2$. Furthermore, all other effects, such as dispersion (essentially electrostatic in character), details of the short range interacting vibrational force field and Jahn–Teller distortions are discussed in the text. It is shown that the overall agreement between our theoretical predictions and experiment is satisfactory for both the relative vibronic intensities and the total oscillator strengths for a set of selected transitions. We also discuss the most likely sources for improvement.

2. Experimental section

2.1. Preliminary remarks

There is a vast amount of experimental data for both pure and doped stoichiometric elpasolite systems [1–3]. The experimental data available is, in general, of good quality and fairly accurate and has been obtained from linear and non-linear optic techniques. In this work, we aim to further test the applicability and flexibility of our current model calculations: vibronic crystal field-closure-ligand polarization (VCF-closure-LP) model. We also have proceeded to examine the controlled synthesis and to study both the structural and spectroscopic characterizations of the neat elpasolite $Cs_2NaTmCl_6$. We report, therefore, new and updated data which will be employed to undertake studies on both the electronic and the vibrational factors, upon which the spectral intensities observed in the luminescence spectra depend upon [4–9]. The mechanistic aspects related to the rates of decay for radiative transitions in systems such as Cs_2NaLnZ_6, where ($Z^- = F^-, Cl^-$) are of our interest and explicit calculations involving these highly relativistic heavy ions have already been performed [1, 10–12] and some further work, taking a broader view, is needed in order to include both the short and the long range interaction terms and in the dynamic matrix [12–20]. In this paper, and for this

system, we have generalized our previous calculations [12–14] and have also included explicit calculations for both absorptions and emissions, for which there is a wealth of well-resolved experimental data. It is essential in any physical model and calculation method to have a database of a high quality and accuracy and we therefore decided to update our structural data and spectroscopic information (mainly from Raman spectroscopy) in order to test the validity and flexibility of our model calculations. In this article, the calculation will be based upon the assumption that the coupling among the internal and the external vibrations is negligible [4–6]. Applications of our formalisms to neat lattices are being performed in our laboratories with reference to the stoichiometric elpasolite-type systems.

2.2. Synthesis and structural characterization

The neat $Cs_2NaTmCl_6$ elpasolite has been synthesized and characterized by means of X-ray powder diffraction and spectroscopic studies. The synthesis took place using a solid state reaction at 802.9°C for a period of two hours with the temperature gradient of 4°C/min and 2°C/min, at the beginning and at the end of the chemical reaction, respectively. Also thermal studies (DTA/TG) were performed to establish the optimum crystallization temperature, and it was found that this occurs from 764.5°C to 838.5°C. The profile refinement computing programs, according to the Rietveld method, allowed us to determine a set of crystallographic parameters to be as: $a_0 = 10.6866$ Å, $V = 1220.45$ Å^3, $Z = 4$, $M = 802.90$, $D_X = 3.65$ and $D_{\exp} = 3.67$. Thirty two experimental lines were analyzed and turn out to be very accurate ($R_{\exp} < R_{\mathrm{wp}}$). For the structure of this elpasolite, cubic closed packed of the form $Cs^+ + 3Cl^-$ are observed and six Cl^- anions are octahedrally bonded to both Tm^{3+} and Na^{3+} ions, while the remaining Cs^+ ions have a coordination number of 12 with respect to the Cl^- ions and lie in the tetrahedral holes of this lattice. Also Raman spectra were taken for this crystal and the odd parity vibrational modes; $\nu_1(\alpha_{1g}, S_1) = 228$, $\nu_2(\epsilon_g, S_2) = 225$, and $\nu_5(\tau_{2g}, S_4) = 130.5$ were assigned and identified. Throughout the synthesis procedure, stoichiometric quantities of CsCl, NaCl, and $TmCl_3$ were dissolved in diluted HCl acid. The obtained product was dried out in a vacuum stove and in a dried N_2-atmosphere in order to perform (DTA/TG) studies so as to obtain the optimum temperature for the thermal analysis, the phase changes and the temperature crystallization range. Figure 1 shows the DTA/TG and it is observed that the range for the crystallization temperatures occurs between 764.5°C and 838.5°C and the maximum of 802.9°C corresponds to the temperature used to carry out the thermal analysis in order to achieve the best possible crystallization. (A mass loss of about 25% may be due to the hydration water currently observed in these highly hygroscopic materials.)

The stoichiometric composition as well as the impurities presence were established by means of X-ray fluorescence and the results obtained are as follows: Tm(25.2%), Cs(39.65%), Na(3.43%), and Cl(31.72%).

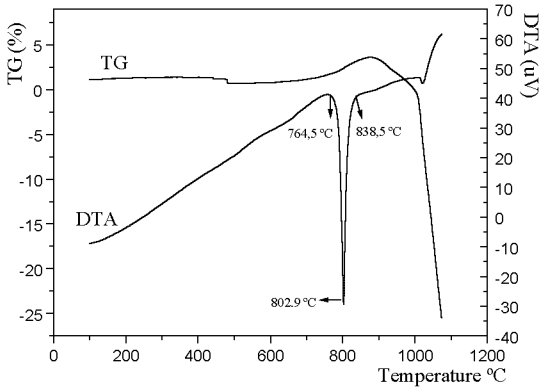

Fig. 1. DTA/TG curves for the elpasolite $Cs_2NaTmCl_6$.

A picnometer LANGER-450, under vacuum, was used to measure the density and we obtained the value of 3.67 g/cm^3.

2.3. Structural and spectroscopic characterization

As we mentioned, in the above section, X-ray powder diffraction studies were carried out and a set of profile refinement computing programs following the Rietveld method was employed. The experimental conditions for the measured system were from 20 mA and 40 kV with a Copper anode and a Ni-filter for a wave length of the incident X-ray of 1.5444 Å. A total of 3149 lines in 0.02°(2θ) steps, at room temperature in the range from 12°(2θ) to 74.98°(2θ), were analyzed. The input data for the profiles refinements are displayed in Table I. We also include the most relevant data from powder diffraction, corresponding to the most relevant lines for this elpasolite (the reader is referred to Table II). Also Fig. 2 displays (at room temperature) the XRD-powder peaks for this neat elpasolite. Besides, and for the sake of completeness, the Raman spectrum of this elpasolite is given in Fig. 3, and the observed even parity Raman active vibrations for the moiety modes of the clusters $TmCl_6^{3-}$ are given in Table III.

TABLE I

Input data and profile refinements.

Factor	Value	Atomic position
R_p	8.48	Cs $\left(\frac{1}{4}, \frac{1}{4}, \frac{1}{4}\right)$
R_{wp}	11.16	Na $\left(\frac{1}{2}, \frac{1}{2}, \frac{1}{2}\right)$
R_{exp}	5.66	Cl $\left(\frac{1}{4}, 0, 0\right)$
R_{wp}/R_{exp}	1.97	Tm (0.0.0)

TABLE II

XRD-powder data.

(h,k,l)	$\frac{I}{I_0}$ (Rietveld)	d(Å) Rietveld	2θ (Rietveld)	$\frac{I}{I_0}$ (Observed)
1,1,1	23	6.16937	14.38077	18
2,0,0	< 1	5.34330	16.61867	< 1
2,2,0	100	3.77878	23.58310	100
3,1,1	19	3.22201	27.73343	20
2,2,2	34	3.08415	28.99964	38
4,0,0	90	2.67165	33.60037	90
3,3,1	10	2.45151	36.72036	11
4,2,0	< 1	2.38952	37.70841	< 1
4,2,2	67	2.18114	41.46863	70
5,1,1 : 3,3,3	9	2.05717	44.09437	12
4,4,0	67	1.83596	49.74462	72
5,3,1	12	1.80604	50.62629	15
4,4,2 : 6,0,0	< 1	1.78146	51.37528	< 1
6,2,0	45	1.68955	54.39315	50
5,3,3	5	1.62971	56.56596	6
6,2,2	18	1.61154	57.26228	20
4,4,4	30	1.54208	60.09956	34
7,1,1 : 5,5,1	5	1.49612	62.14671	6
6,4,0	< 1	1.48223	62.79492	< 1
6,4,2	61	1.42773	65.48421	61
7,3,1 : 5,5,3	9	1.30140	67.41876	8

TABLE III

Observed Raman vibrational frequencies.

Symmetry species	Assignment	Active	ν (cm^{-1})	Intensity
$\alpha_{1g}(\nu_1)$	ν (Tm–Cl)	Raman	288	s
$\varepsilon_g(\nu_2)$	ν (Tm–Cl)	Raman	225	w
$\tau_{2g}(\nu_5)$	δ (Cl–Tm–Cl)	Raman	130.5	s

Finally, it is shown that the average atomic positions for the nuclei ions are: Tm(0,0,0), $4Na^+(\frac{1}{2},\frac{1}{2},\frac{1}{2})$, $8Cs^+(\frac{1}{4},\frac{1}{4},\frac{1}{4})$ and $24Cl^-(\frac{1}{4},0,0)$ and the lattice parameter was found to be $a_0 = 10.6866$ Å.

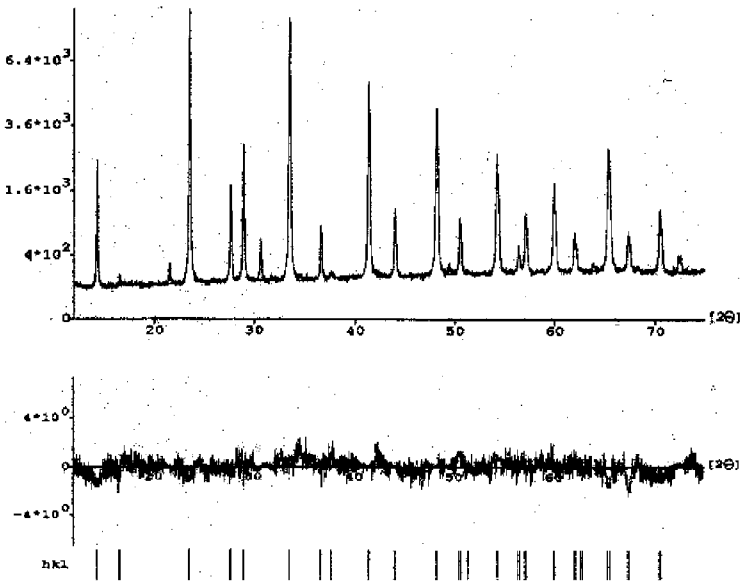

Fig. 2. XRD-powder. Rietveld refinement.

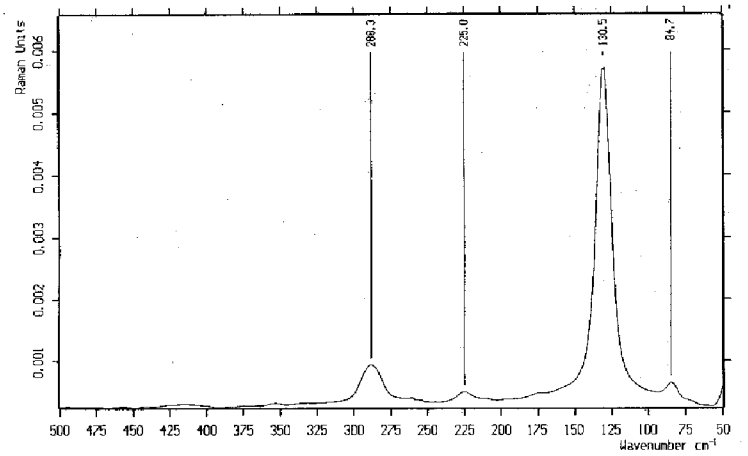

Fig. 3. Raman spectrum for the elpasolite $Cs_2NaTmCl_6$.

3. Theoretical section

3.1. Introduction

The energy levels for the $TmCl_6^{3-}$ ions in $Cs_2NaTmCl_6$ have been the subject of many discussions in the literature [21], mainly due to calculated values for σ_{rms} (between the observed and calculated energies) using different model Hamiltonians [22, 23]. A vast amount of experimental data for systems such as Cs_2NaTmZ_6

with $Z^- = Br^-$ and Cl^- are available in the literature [1, 11, 24]. A thorough experimental study was performed by Tanner et al. [25] for this system and the energy levels corresponding to the $^3H_5$ multiplets were reassigned by utilizing updated experimental data from infrared absorption experiments. Similarly, the electronic Raman spectrum is supplied with new information that helps to resolve the discrepancies concerning the state $|(^3H_6)\Gamma_2\rangle$. Also the coupling between the energy levels $|(^3H_6)a\Gamma_5\rangle$ and $|(^3H_6)\Gamma_1\rangle + \nu_5(\Gamma_5)$ give rises to two energy levels, and one of them was previously assigned to the Γ_2-symmetry. A tentative new assignment has been proposed in Ref. [25]. It was also possible to locate, from the absorption spectra, the energy levels of Γ_4-symmetry, which may be found at higher energies. In spite of all the refinements reported by these authors, the value for the root mean square deviation remains: $\sigma_{\mathrm{rms}} = 32.50\ \mathrm{cm}^{-1}$. For the elpasolite-type systems, there are several classic papers in the literature [26 and references therein], where these authors using data from absorption worked out an energy levels ordering. Also some intensity calculation were performed for $f \rightarrow f$ transitions, involving the terminal states $|(^3H_6)\Gamma\rangle \rightarrow |(^4H_4)\Gamma'\rangle, |(^3F_3)\Gamma''\rangle, |(^3F_2)\Gamma'''\rangle, |(^1G_4)\Gamma'\rangle$, and $|(^1D_2)\Gamma'''\rangle$; $\Gamma = \Gamma_1, \Gamma_2, \Gamma_3, \Gamma_4, {}^a\Gamma_5, {}^b\Gamma_5$; $\Gamma' = \Gamma_1, \Gamma_3, \Gamma_4, \Gamma_5$; $\Gamma'' = \Gamma_2, \Gamma_4, \Gamma_5$, and $\Gamma''' = \Gamma_3, \Gamma_5$. In spite of all these efforts, the quality and insight of these results, obtained by Richardson et al. [22, 23, 26], are modest and new and updated intensity models are required.

For the stoichiometric elpasolites, it does seem that Tanner et al. [27, 28] has managed to collect the more complete and comprehensive database. The absorption spectra for $Cs_2NaTmCl_6$ has been measured and recorded at 20 K and 85 K. Similarly, the spectra for the elpasolites of Gd [28] and Ho [27] doped with $TmCl_6^{3-}$ ($\simeq$ 1 mol% of Tm^{3+}), have also been measured at the temperatures of 20 K and 300 K. The analysis of the spectrum associated with $Cs_2NaGdCl_6$:$TmCl_{6,}^{3-}$ allowed these authors to detect emission from the $|(^1G_4)\Gamma'\rangle$ and to identify and assign the various emissions: $^1G_4\Gamma' \rightarrow {}^3H_6\Gamma$, $^3F_4\Gamma'$, $^3H_5\Gamma''''$ with $\Gamma'''' = \Gamma_3$, ${}^a\Gamma_1$, ${}^b\Gamma_4, \Gamma_5$. In Ref. [27] the reminiscence spectra corresponding to the emissions $^3H_4\Gamma' \rightarrow {}^3H_6\Gamma$ at 20 K is reported in the energy region from the 12,600 to 11,800 cm^{-1}, using an Ar laser (474 nm line). At 20 K the luminescence detected was rather weak to be used for a thorough analysis of these emissions. A subsequent work of Tanner [24] informed the infrared luminescence spectrum at liquid N_2 at the temperature of 85 K with a resolution of about 5 to 10 cm^{-1}, using an Ar laser (476 nm line). Several emissions were analyzed such as $^3H_4\Gamma' \rightarrow {}^3F_4\Gamma'$, $^3H_5\Gamma''''$ and $^3F_4\Gamma' \rightarrow {}^3H_6\Gamma$.

Further studies [1, 29] have been carried out to fit the energy level parameters to the experimental data, based upon this more complete and comprehensive database, which was performed for the series of the lanthanide in stoichiometric elpasolites. Due to the observed wealth of the vibronic structure for the Tm(III) hexachloride-elpasolite, we have decided to investigate both the emissions $^3H_4(\Gamma_i) \rightarrow {}^3F_4(\Gamma_j)$ and the absorptions $^3H_6(A_1) \rightarrow {}^3F_4(\Gamma_i)$, $^1G_4(\Gamma_i)$, $^3H_5(\Gamma_l)$,

with Γ_k $(k = i, j) = A_1, E, T_1, T_2$ and $\Gamma_l = E$, ${}^aT_1$, ${}^bT_1, T_2$. We will show that the overall agreement between our theoretical predictions and the experiment is satisfactory and the most likely sources for improvement will be also discussed in the coming sections. The unit cell for these elpasolite is given in Fig. 4. It is seen from

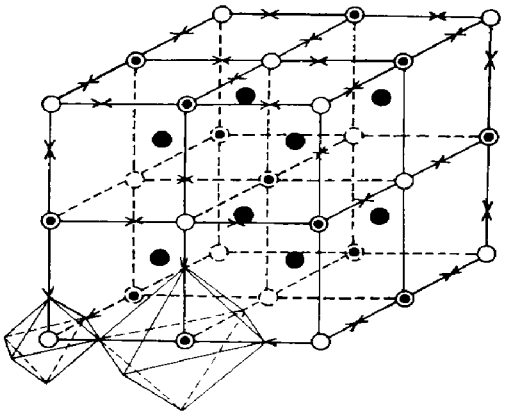

Fig. 4. Unit cell.

this structure that the site symmetries for Na^+, Cs^+, and $TmCl_6^{3-}$ are O_h, T_d, and O_h, respectively. The complexity of the experimental information provided by the absorptions and the emissions is such that the actual evaluation of spectral intensities is a truly formidable task to achieve. Several elements should be taken into account if one wishes to gain understanding in these complex radiate processes: (a) Most likely mechanisms to account for the observed intensities in both absorptions and emissions. The role played by the intermediate electronic states. (b) A sensible description of the electronic states for which a full configuration interaction method is introduced. (c) A more accurate and sound description for the normal modes of vibrations of the systems is required. Inclusion of both short and long range interaction terms is required and (d) an analytical study of the vibronic line shapes and potential energy surfaces must be considered.

3.2. Energy levels for $TmCl_6^{3-}$ complex ion in $Cs_2NaTmCl_6$

The Tm(III) ion corresponds to a $4f^{12}$ free ion electronic configuration, and therefore a total of 91 microstates, compatible with the Pauli Principle, may be written. These zero-order free ion wave functions are eigenfunctions of the mono-electronic effective Hamiltonian $\widehat{H}^0 = \sum_{i=1-12} \left\{ -\frac{\hbar^2}{2m}\nabla_i^2 - \frac{Z_i e^2}{r_i} \right\}$. For a system such as $TmCl_6^{3-}$, the simplest model Hamiltonian to introduce is the following:

$$\widehat{H} = \widehat{H}^0 + \sum_{i<j} \frac{e^2}{r_{i,j}} + \sum_i \xi(r_i)(\boldsymbol{l}_i \cdot \boldsymbol{s}_i) + V(O_h) \tag{1}$$

and for f-electrons, the effective crystal field potential may be written as given below:

$$V(O_h) = \left\{ \frac{7}{2} C_0^{(4)} + \frac{\sqrt{70}}{4} (C_{+4}^{(4)} + C_{-4}^{(4)}) \right\} B_4$$

$$+ \left\{ \frac{3}{4} C_0^{(6)} - \frac{3\sqrt{14}}{8} (C_{+4}^{(6)} + C_{-4}^{(6)}) \right\}. \tag{2}$$

Here $B_k = e^2 \langle r^k \rangle / R_0^{k+1}$, R_0 is identified with the Ln–Cl bond distance, $\langle r^k \rangle$; $k = 4, 6$ is the expectation value of r^k, when evaluated within the manifold of $4f$-SCF-radial states and $C_q^{(k)} = \sqrt{4\pi/(2k+1)} Y_{k,q}(\theta, \phi)$ are the standard tensor operator of rank k. For the radial expectation values reported by Judd† [30] and also for $R_0 = 2.69 \times 10^{-8}$ cm we obtain $(B_4/B_6) \simeq 5.56$.

Having reached this point in the discussion, let us underline that our strategy will be to avoid an excessive parameterization in the energy level calculation, simple because our database is not large enough to accommodate such a lot of both relativistic and nonrelativistic parameters in the model Hamiltonian for the system [1, 5, 6, 14, 22, 23, 26]. We believe that these full parameterization procedures obscure both the physics and the chemistry of the problem we aim to solve, therefore we will work on a model based upon a minimum set of parameters to be fitted from experiment. Thus, in this model we will employ a model Hamiltonian as given above in Eq. (1). This implies that in our model Hamiltonian terms such as orbit–orbit and orbit–other orbit, etc.,..., will be excluded as well as effects such as electron transfer and other ones related to it. The calculation will be carried out on the basis of a seven-atom system approximation and within the independent system model (ISM). When these approximations are adopted, we assume that the coupling among the internal $TmCl_6^{3-}$ and the lattice vibrations is small and/or negligible. We also assume that the total transition dipole moment may be partitioned into two contributions, one of them derived from the vibronic crystal field (CF) and the other one from the vibronic ligand polarization (LP) models. It is obvious that when the ISM is used, then we assume that there is no overlap between the central ion and the ligand sub-systems charge densities. Thus, we write the identify

$$\boldsymbol{\mu}_{1\to 2} = \boldsymbol{\mu}_{1\to 2}^{\mathrm{CF}} + \boldsymbol{\mu}_{1\to 2}^{\mathrm{LP}} \tag{3}$$

and therefore, the total dipole strength associated with the $|1\rangle \to |2\rangle$ excitation becomes

$$D_{1\to 2} = D_{1\to 2}^{\mathrm{CF}} + D_{1\to 2}^{\mathrm{LP}} + D_{1\to 2}^{(\mathrm{CF,LP})}, \tag{4}$$

where the interference term is defined as follows:

$$D_{1\to 2}^{(\mathrm{CF,LP})} = \langle 0 | \boldsymbol{\mu}_{1\to 2}^{\mathrm{CF}^*} \boldsymbol{\mu}_{1\to 2}^{\mathrm{LP}} + \boldsymbol{\mu}_{1\to 2}^{\mathrm{LP}^*} \boldsymbol{\mu}_{1\to 2}^{\mathrm{CF}^*} | 1 \rangle. \tag{5}$$

† $\langle r^2 \rangle = 0.761 a_0^2$, $\langle r^4 \rangle = 1.570 a_0^4$, $\langle r^6 \rangle = 7.310 a_0^6$ with $a_0 = 0.529$ Å.

It is interesting to observe that the above identity has been written under the basic assumption that the potential energy surfaces of the two terminal electronic states have roughly the same shape and are only vertically displaced to one another, along the totally symmetric normal modes of vibration (breathing mode of α_{1g}-symmetry). A careful look at the model Hamiltonian and the effective crystal field potential leads us to the conclusion that for the energy level calculation the parameters F_2, F_4, F_4, ξ_{so}, B_4, and B_6 are required to be fitted from the experimental data (the F_0-parameter has been excluded since the experimental data is refereed to energy differences ΔE, and therefore in all our energy matrices may be cancelled out). It is customary, in the literature [31], to use the parameters introduced by Racah E^k; $k = 0, 1, 2, 3$, which are expressed as linear combinations of the electron–electron repulsion parameters F_k; $k = 0, 2, 4, 6$. We use the transformations: $E^0 = F_0 - 10F^2 - 35F_4 - 286F_6$, $E^1 = \frac{1}{9}(70F_2 + 231F_4 + 2002F_6)$, $E^2 = \frac{1}{9}(F_2 - 3F_4 + 7F_6)$, $E^3 = \frac{1}{3}(5F_2 + 6F_4 - 91F_6)$. In our current six-parameter model, a set of representative values (not the best fit) is as follows: $E^0 = -8,783$, $E^1 = +6,831$, $E^2 = +34$, $E^3 = +683$, $\xi_{so} = +2,624$, $B_4 = +385$, and $B_6 = +69$. All these values are given in cm^{-1}. In a previous and preliminary research work [14], we published three different sets of wave functions using various levels of approximation and models of six and ten parameters. The details of these calculations may be obtained upon request from R.A.

3.3. Theoretical model. Spectral intensities in absorptions and emissions

The vibronic intensity calculations were carried out, using a generalization of the vibronic crystal field-closure-ligand polarization model (VCF-closure-LP). Here, we will give a brief summary of the relevant identities involved in the calculation. Extensive tabulations required to undertake this calculations will not be included, though they are available upon request from R.A.

3.3.1. Vibronic crystal field contribution to the total transition dipole moment

The crystal field contribution to the overall transition dipole moment associated with the excitation $|1\rangle \longrightarrow |2\rangle$ is as given below:

$$\mu_{1\longrightarrow 2}^{\mathrm{CF},\alpha}(\nu_t) = \sum_m \langle 1|U_{\nu_m}^{\mathrm{CF},\alpha}|2\rangle L_{mt}\langle 0|Q_{\nu_t}|1\rangle, \tag{6.1}$$

where

$$\langle 1|U_{\nu_m}^{\mathrm{CF},\alpha}|2\rangle = \sum_\Gamma \sum_k C_k^{\mathrm{CF}}(-1)^{\Gamma_1+\gamma_1^+} V \begin{pmatrix} \Gamma_1 & \Gamma_2 & \Gamma \\ \gamma_1^+ & \gamma_2 & \gamma \end{pmatrix}$$

$$\times \langle (LSJ)\Gamma_1|O_{\nu_t}^{\Gamma}(k,\tau)|(L'SJ')\Gamma_2\rangle A_{\nu_t}^{\Gamma\gamma}(k-1,\tau) \tag{6.2}$$

and also

$$A_{\nu_t}^{\Gamma\gamma}(i,\tau) = \sum_L \left\{ \frac{\delta G_{\Gamma\gamma}^{\mathrm{CF},L}(i,\tau)}{\delta S_{\nu_t}} \right\}_0 \quad \text{and} \quad C_k^{\mathrm{CF}} = \frac{2e}{\Delta E}\langle \gamma_k \rangle, \tag{6.3}$$

where $\langle\gamma_k\rangle = e^2\langle r^k\rangle/R_0^{k+1}$. The notation employed in Eqs. (6.1–6.3) has been given in several references [5, 6, 12, 13– 15, 18–20, 32–36 and references therein]. For the sake of completeness, we observe that the transition dipole moment corresponds to the expectation value of the product between an electronic factor U and a vibrational factor Q. In the current notation Q stands for the matrix of the normal coordinates of the system. Furthermore, the elements of the L-matrix relate the symmetry coordinates to the normal coordinates by means of the relationship: $S = LQ$. Also, the crystal field vibronic coupling constants are labelled as A, see Eq. (6.3). The reader is referred, in particular to Ref. [33] for further details. Full tabulation of the above quantities (6.1–6.3) may be obtained upon request from R.A.

3.3.2. Vibronic ligand polarization contributions to the total transition dipole moments

The α-th component of the ligand polarization electric dipole moment associated with the $|1\rangle \longrightarrow |2\rangle$, electronic transition is written as given by Eq. (6.1), where CF must be replaced by LP for the sake of completeness. Do observe that the transition dipole moment is referred to the excitation $\Gamma_1 \longrightarrow \Gamma_2 + \nu_t$. Next, we define the ligand polarization vibronic coupling constants as follows:

$$B_{\Gamma\bar{\gamma}}^{\Gamma\gamma,\alpha}(k,t) = \sum_L \left\{ \frac{\delta G_{\Gamma\gamma,\alpha}^{\mathrm{LP},L}(k)}{\delta S_{\bar{\gamma}}^{\Gamma}(t)} \right\}_0 \tag{7.1}$$

and it is straightforward to show that the ligand polarization electronic factors, associated with the $\Gamma_1 \longrightarrow \Gamma_2 + \nu_t$ transition may be written as follows:

$$U_{\nu_t}^{\mathrm{LP},\alpha} = \sum_L \sum_k C_k^{\mathrm{LP}} (-1)^{\Gamma_1+\gamma_1^+} V \begin{pmatrix} \Gamma_1 & \Gamma_2 & \Gamma \\ \gamma_1^+ & \gamma_2 & \gamma \end{pmatrix}$$
$$\times \langle (LSJ)\Gamma_1 | M_{\nu_t}^{\Gamma}(k) | (L'SJ')\Gamma_2 \rangle B_{\nu_t}^{\Gamma\gamma,\alpha}(k,t), \tag{7.2}$$

where $C_k^{\mathrm{LP}} = \left(\alpha_L \langle r^k\rangle / R_0^{k+3}\right) e$. It is seen that Eq. (7.1) is employed to introduce the vibronic ligand polarization, vibronic coupling constants, and the electronic factor, within the framework of the vibronic ligand polarization model, is given in full in Eq. (7.2). Full tabulations of the above quantities (7.1), (7.2) may be obtained upon request from R.A.

3.4. Results

As it was pointed out earlier in the text, the intensity calculation were carried out within the framework of the independent system model and the seven-atom system approximation (the long range interactions due to Coulombic terms have been excluded, and therefore the coupling among the internal and the external lattice vibrations has been assumed either too small or negligible). A view of the details and approximations involved in these calculations may be found in several references [5, 6, 9, 12–14, 19, 20, 32–35] and we will not repeat them here. Next,

in Table IV, we report the observed and the calculated energy levels (six-energy parameter model) and to a maximum extent we have avoided the over parameterization of the model Hamiltonian. We must bear in mind that only very rarely a fairly complete set of data is available for these types of systems [5, 13–15], and therefore it seems appropriate to test our models and their predictions against the experimental data. This system is in a way rather unique since we have done full length calculations for both absorptions and emissions to get more physical insight. For the sake of simplicity, we list only a representative set of wave functions. The actual composition of them is available upon request from R.A.

TABLE IV

Wave functions, observed and calculated energies (cm^{-1}).

States	Energy (obs.)	Energy (cal.)
$^3H_6\Gamma_1$	0	0
$^3F_4\Gamma_5$	5.547	5.553
$^3F_4\Gamma_3$	5.814	5.791
$^3F_4\Gamma_4$	5.866	5.858
$^3F_4\Gamma_1$	5.938	5.952
$^3H_5\ ^b\Gamma_4$	8.241	8.251
$^3H_5\Gamma_3$	8.270	8.284
$^3H_5\Gamma_5$	8.436	8.462
$^3H_5\ ^a\Gamma_4$	8.532	8.544
$^3H_4\Gamma_5$	12.538	12.530
$^3H_4\Gamma_3$	12.607	12.691
$^3H_4\Gamma_4$	12.840	12.736
$^3H_4\Gamma_1$	12.882	12.844
$^1G_4\Gamma_5$	20.851	20.888
$^1G_4\Gamma_3$	21.256	21.230
$^1G_4\Gamma_4$	21.424	21.320
$^1G_4\Gamma_1$	21.508	21.238

Next, in Tables V and VI, we report the calculated values for the relative vibronic intensity distributions associated with our set of wave functions derived from the six parameters listed above in the text. For all the calculations, we have modelled the normal coordinates of the system, using a general valence type force field [13]. The transformation matrix relating the symmetry coordinates to the normal coordinates, by means of the identity: $S = LQ$, has been worked out and for the odd parity blocks, we obtain: $L_{33} = +0.199761$, $L_{34} = +0.0118683$, $L_{43} = -0.135884$, $L_{44} = +0.292071$, and $L_{66} = +0.237514$. Experimental data of good quality may be found in Ref. [14] with reference only to the absorption

TABLE V

Emissions $|(^3H_4)\Gamma_1\rangle \rightarrow |(^3F_4)\Gamma\rangle$; $\Gamma = \Gamma_1, \Gamma_3, \Gamma_4, \Gamma_5$.

ν_t	Γ_1	Γ_3	Γ_4	Γ_5
	$\|(^3H_4)\Gamma_1\rangle \rightarrow \|(^3F_4)\Gamma\rangle$			
ν_3	1.06×10^{-11}	4.20×10^{-8}	3.06×10^{-12}	5.22×10^{-9}
ν_4	3.39×10^{-10}	3.27×10^{-10}	2.92×10^{-11}	5.42×10^{-10}
ν_6	0	5.46×10^{-9}	1.35×10^{-11}	1.00×10^{-9}
	$\|(^3H_4)\Gamma_3\rangle \rightarrow \|(^3F_4)\Gamma\rangle$			
ν_3	3.86×10^{-8}	5.97×10^{-9}	1.12×10^{-9}	3.49×10^{-9}
ν_4	3.00×10^{-10}	5.35×10^{-11}	6.92×10^{-10}	3.80×10^{-10}
ν_6	5.03×10^{-9}	1.63×10^{-9}	7.69×10^{-10}	1.39×10^{-9}
	$\|(^3H_4)\Gamma_4\rangle \rightarrow \|(^3F_4)\Gamma\rangle$			
ν_3	2.91×10^{-12}	1.18×10^{-9}	7.86×10^{-9}	6.66×10^{-10}
ν_4	2.77×10^{-11}	7.31×10^{-10}	6.82×10^{-11}	1.91×10^{-9}
ν_6	1.28×10^{-11}	8.11×10^{-10}	9.57×10^{-9}	2.36×10^{-9}
	$\|(^3H_4)\Gamma_5\rangle \rightarrow \|(^3F_4)\Gamma\rangle$			
ν_3	4.26×10^{-9}	3.14×10^{-9}	5.55×10^{-10}	3.20×10^{-10}
ν_4	4.67×10^{-10}	3.53×10^{-10}	1.61×10^{-9}	2.12×10^{-9}
ν_6	8.50×10^{-10}	1.25×10^{-9}	1.99×10^{-9}	2.87×10^{-9}

TABLE VI

The absorptions $|(^3H_6)\Gamma_1\rangle \rightarrow |(^3F_4)\Gamma_i\rangle$, $|(^1G_4)\Gamma_i\rangle$, $|(^3H_5)\Gamma_l\rangle$ with $\Gamma_i = \Gamma_1, \Gamma_3, \Gamma_4, \Gamma_5$ and $\Gamma_l = \Gamma_3, {}^a\Gamma_4, {}^b\Gamma_4, \Gamma_5$.

ν_t	Γ_1	Γ_3	Γ_4	Γ_5
	$\|(^3H_6)\Gamma_1\rangle \rightarrow \|(^3F_4)\Gamma\rangle$			
ν_3	6.43×10^{-11}	2.39×10^{-8}	5.96×10^{-13}	2.39×10^{-8}
ν_4	1.96×10^{-9}	3.56×10^{-10}	1.63×10^{-11}	5.89×10^{-9}
ν_4	0	1.01×10^{-9}	9.04×10^{-13}	9.79×10^{-9}
	$\|(^3H_6)\Gamma_1\rangle \rightarrow \|(^1G_4)\Gamma\rangle$			
ν_3	2.30×10^{-11}	7.22×10^{-9}	5.51×10^{-13}	8.47×10^{-9}
ν_4	7.11×10^{-10}	1.18×10^{-10}	1.53×10^{-11}	2.10×10^{-9}
ν_4	0	2.57×10^{-10}	8.53×10^{-13}	3.73×10^{-9}
	$\|(^3H_6)\Gamma_1\rangle \rightarrow \|(^3H_5)\Gamma\rangle$			
ν_3	2.74×10^{-8}	1.00×10^{-11}	4.14×10^{-12}	3.60×10^{-9}
ν_4	1.66×10^{-10}	2.75×10^{-10}	1.14×10^{-10}	5.39×10^{-10}
ν_4	4.10×10^{-9}	1.53×10^{-11}	6.33×10^{-12}	8.57×10^{-10}

spectrum for this system. It is indeed very challenging to test the validity of our calculated spectral intensities against the experimental data, bearing in mind the

approximations involved in our model calculation. In spite of these limitations, we have to conclude that the calculated values for the overall oscillator strengths in both absorption and emission are in remarkable agreement with experiment.

Deviation from the experimental data may be observed in the absorption spectrum for this elpasolite, regarding the relative vibronic intensity distributions for various electronic transitions. Several reasons have been given to account for these deviations, however we have solid evidence that the role played by the normal modes, including the coupling among the internal and the external vibrations is a major cause of these deviations. It is therefore advisable to consider full lattice dynamic calculations, including both the short and the long range interactions in the crystal. The work in this direction is in progress in our laboratory.

4. Discussion

When these results are tested against the experimental data (when available), see Refs. [1, 13, 14, 19–22, 24, 25, 27, 28, 36] it is generally found that the calculated overall oscillator strengths agree fairly well with those reported in the literature. It is also observed that there is a particular distribution of the intensities due to the three false origins, from transition to transition, and there are cases where this simple model calculation cannot reproduce satisfactorily the observed vibronic intensity distribution $f(\nu_3) : f(\nu_4) : f(\nu_6)$. There are though some mechanistic aspects which require more work. We may also anticipate several sources for improvements of our intensity model. (a) The actual coupling among the internal and the external modes must be taken into account. Also, the long range interaction terms, mainly Coulombic in character, should be included. (b) The quality of the wave functions used in the calculation must be reviewed and there is an urgent need to incorporate excited states of the lanthanide ions. (c) The closure approximation needs to be relaxed and explicit inclusion of intermediate states is needed and (d) we need to consider the mixing of vibronic states belonging to the same irreducible representation with energy very closed to each other and that in principle may involve the same vibronic origins. In spite of the above limitations, which should be lifted it is seen that our model calculation is both useful and flexible and can be applied to these complex radiative processes with a fair degree of success. Calculations in similar systems are also in due course in our laboratories. A close look at Ref. [14] indicates that for the absorptions, the overall oscillator strengths for the various excitations considered in this work, agree remarkably well with experiment and only for some individual vibronic origins (when considered individually) deviations from experiment become important. This is not a reason for concern, since it must be said that the model calculation used in the present research work is suitable to accommodate vibronic intensities due to each and all of the vibronic origins, so as to provide each vibronic transition an estimation of the intensity ratios $f(\nu_3) : f(\nu_4) : f(\nu_6)$.

Acknowledgment

R.A. would like to express his gratitude to Fondecyt, grant 1981207, the Universidad Diego Portales, grant VRA 2049 and to the Institute of Low Temperature and Structure Research, Polish Academy of Sciences, Wrocław, Poland for the hospitality and the right environment provided (February, 2001). We would also like to acknowledge Prof. R. Tabensky for many highly illuminating discussions and a careful reading of the manuscript.

References

[1] P.A. Tanner, V.V.R.K. Kumar, C.K. Jayasankar, M.F. Reid, *J. Alloys Comp.* **215,** 349 (1994).

[2] F. Auzel, in: *Proc. Int. Conf. Defects Insulating Materials*, Nordkirchen, World Scientific, Singapure 1993.

[3] G. Blasse, B.C. Grabmaier, *Lumiscent Materials*, Spring Verlag, 1994.

[4] R. Acevedo, V. Poblete, *Powder Diffraction* **10,** 241 (1995).

[5] R. Acevedo, P.A. Tanner, T. Meruane, V. Poblete, *Phys. Rev. B* **54,** 3976 (1996).

[6] R. Acevedo, C.D. Flint, T. Meruane, G. Munoz, M. Passman, V. Poblete, *J. Mol. Struct. (Theochem)* **390,** 109 (1997).

[7] R. Acevedo, *Prensa Cientifica S.A.*, in press.

[8] C.J. Ballahausen, *Vibronic Processes in Inorganic Chemistry*, NATO-ASI, Series C: *Mathematical and Physical Sciences*, Vol. 288, Kluwer Academic Publishers, Dordrecht 1989, p. 1, 53.

[9] R. Acevedo, *Vibronic Processes in Inorganic Chemistry*, NATO-ASI, Series C: *Mathematical and Physical Sciences*, Vol. 288, Kluwer Academic Publishers, Dordrecht 1989, p. 139.

[10] B. Nissen, T. Luxbacher, W. Strek, C.D. Flint, *Chem. Phys. Lett.* **303,** 235 (1999).

[11] B. Nissen, W. Strek, C.D. Flint, submitted to *Chem. Phys. Lett.*

[12] O. Hurtado, R. Acevedo, T. Meruane, *Rev. Mex. Fis.* **44 S1,** 44 (1998).

[13] O.F. Hurtado, M.Sc. Thesis, Universidad de Chile, 2000.

[14] P.A. Tanner, R. Acevedo, O. Hurtado, T. Meruane, *J. Alloys Comp.* **323-324,** 718 (2001).

[15] R. Acevedo, *Elementos Introductorios en Espectroscopia Atomica y Molecular, Aplicaciones a Sistemas de Interes Espectroscopico*, RIL Editores, ISBN: 956-284-164-4, Santiago-Chile 2000.

[16] A. Lentz, *J. Chem. Phys. Solids* **35,** 827 (1974).

[17] A.D. Cracknell, *Group Theory in Solid State Physics*, Taylor and Francis Ltd. London, Halsted Press, London 1975.

[18] D.I. Torres, J.D. Freire, R.S. Katiyar, *Phys. Rev. B* **56,** 7763 (1997).

[19] R. Acevedo, T. Meruane, G. Navarro, W. Strek, Part I, submitted to *J. Mol. Struct.*

[20] R. Acevedo, T. Meruane, G. Navarro, W. Strek, Part II, submitted to *J. Mol. Struct.*

[21] P.A. Tanner, *J. Chem. Phys.* **85,** 2344 (1986).

[22] F.S. Richardson, M.F. Reid, J.J. Dallara, R.D. Smidth, *J. Chem. Phys.* **83,** 3813 (1985).

[23] D.R. Foster, M.F. Reid, F.S. Richardson, *J. Chem. Phys.* **83,** 3225 (1985).

[24] P.A. Tanner, *Mol. Phys.* **54,** 883 (1985).

[25] P.A. Tanner, T.K. Choi, K. Hoffman, *Appl. Spectrosc.* **47,** 1084 (1993).

[26] R. Schwartz, T. Faulkner, F.S. Richardson, *Mol. Phys.* **38,** 1767 (1979).

[27] P.A. Tanner, *Mol. Phys.* **53,** 813 (1984).

[28] P.A. Tanner, *Mol. Phys.* **53,** 835 (1984).

[29] P.A. Tanner, V.R.K. Kumar, C.K. Jayasankar, M.F. Reid, *J. Alloys Comp.* **225,** 85 (1995).

[30] B.R. Judd, *Phys. Rev.* **127,** 750 (1962).

[31] E.U. Condon, G.H. Shortley, *The Theory of Atomic Spectra*, Cambridge University Press, Cambridge 1967.

[32] R. Acevedo, G. Navarro, T. Meruane, P.A. Tanner, Y.Y. Zhao, *Rev. Mex. Fís.* **47,** 245 (2001).

[33] R. Acevedo, T. Meruane, G. Navarro, *Acta Phys. Pol. A* **99,** 233 (2001).

[34] R. Acevedo, E. Cortés, submitted to *Theoretical Chemistry Accounts.*

[35] R. Acevedo, O.F. Hurtado, V. Poblete, J. Pozo, R. Elgueta, P.A. Tanner, *Nucleotécnica*, Año 20, No. 34, 39(2000).

[36] P.A. Tanner, *J. Chem. Soc. Faraday Trans. II* **81,** 1285 (1985).